Synthesis and Characterization of Cadmium Doped Nickel Ferrite ($Ni_{0.6}Cd_{0.4}Fe_2O_4$) Nanoparticles and its Optical Properties

Sandhya Singh, Gaurav Hitkari, G. Pandey

Abstract-Cd-Ni ferrite nanoparticles with a composition of $Ni_{0.6}Cd_{0.4}Fe_2O_4$ have been successfully prepared via simple coprecipitation technique using sodium hydroxide (NaOH) solution is used as a precipitating agent. The structural and optical properties of the samples were studied using Powder X-ray diffraction (PXRD), Scanning electron microscopy (SEM), Energy dispersive X-ray spectroscopy (EDX), Fourier transform Infrared Spectroscopy (FITR), Uv-visible spectroscopy (Uv-vis), and Fluorescence spectroscopy (FL) measurements. The PXRD analysis of all the samples shows the cubic phase without any impurity peaks. The average particle sizes were calculated by Scherrer's formula. The SEM image shows the agglomeration and flakes type nanoparticles with many void spaces due to exhaust of gases. EDX analysis is used for the elemental analysis of prepared samples (Cd, Ni, Fe, and O). FTIR spectra of the samples show the nature of the chemical bond between metal oxygen bonds (M-O). Uv-vis and FL spectra is used for the band gap calculation and its optical properties.

Keywords: Fluorescence spectroscopy, Nickel ferrite, EDX, SEM, PXRD.

1. INTRODUCTION

Ferrites are unbreakable, fragile, iron containing, gray or black in colour and they are polycrystalline i.e. made up of outsized number of crystals. They are formed by the chemical combination of iron oxide with one or extra other metals. These are ferrimagnetic material which encompasses iron or iron amalgams with body centered cubic crystal structure [1, 2]. Ferric oxide (iron oxide or rust) combined with any number of other metals as well as Mg, Ba, Mn, Ni, Cu or even iron itself. A ferrite is usually represented by the general formula MFe_2O_4 where M represents a few divalent metal that forms divalent bonds, such as elements Mg, Ba, Mn, Ni, Cu or even iron itself. Nickel ferrite for specimen is $NiFe_2O_4$, Manganese ferrite is $MnFe_2O_4$, and both are spinel ferrites. The most familiar ferrite known since biblical times is Magnetite (lode stone or ferrous ferrite $FeFe_2O_4$. Spinel Ferrite are performance a form of magnetism known as ferrimagnetism which is outstanding from the ferromagnetism of such materials as Fe, Co, and Ni [3-5]. The structure of spinels can be 'normal' or 'inverse' is depending on the dissemination of cations on the interstitial sites. In situation the normal spinel, all the tetrahedral (A) sites are occupied by divalent cation, while the octahedral (B) sites are occupied by trivalent cation. Cadmium ($CdFe_2O_4$) and zinc ($ZnFe_2O_4$) ferrites are instances of normal spinels [6-9], where all the Cd^{2+} and Zn^{2+} ions are dispersed on the A sites and the Fe^{3+} ions occupy the B sites. In the situation inverse spinel structure the trivalent cation are dispersed similarly between A and B sites whilst all the divalent ions occupy B sites. Copper ($CuFe_2O_4$) and nickel ($NiFe_2O_4$) ferrites are instances of inverse spinels [10, 11]. In general, the dissemination of the different ions (cations) in the tetrahedral and octahedral sites of the spinel ferrite lattice essentially be influenced by the method of preparation and the processing situations. Innumerable preparation methods; for instance chemical co-precipitation, technique have been technologically advanced to produce nanosized ferrite nanoparticles. Nickel ferrite ($NiFe_2O_4$) nanoparticles is

- *Sandhya Singh pursuing Ph.D degree in Department of Applied Chemistry in Babasaheb Bhimrao Ambedkar University, Lucknow. E-mail: sandhyacsjm011@gmail.com*
- *Gaurav Hitkari pursuing Ph.D degree in Department of Applied Chemistry in Babasaheb Bhimrao Ambedkar University, Lucknow.*
- *G. Pandey Associate Professor Department of Applied Chemistry in Babasaheb Bhimrao Ambedkar University, Lucknow.*

unique lenient ferrite material owing to its low conductivity [12], lower eddy current fatalities and high electrochemical steadiness [13] with inverse spinel structure. The properties of nickel ferrite are, to a great extent, used in technological applications, as well as telecommunication, memory devices, electronic devices, antenna and transformer cores [14].

In the present work, $Ni_{0.6}Cd_{0.4}Fe_2O_4$ nanoparticles with a composition have been effectively synthesized via chemical coprecipitation technique using sodium hydroxide as precipitating agent. Advantage of this method is product formed is multi-component materials very effortlessly without any contaminations with desired stoichiometry. With this technique, particle size, chemical uniformity and degree of agglomeration can be without difficulty controlled. The prepared samples were characterized using Powder X-ray Diffraction (PXRD), Scanning Electron Microscopy (SEM), Energy dispersive X-ray spectroscopy (EDX), Fourier Transform Infrared Spectroscopy (FTIR), Uv-visible spectroscopy (Uv-vis) and Fluorescence spectra (FL).

2. EXPERIMENTAL SECTION

2.1 Materials

For the synthesis of $Cd_{0.4}Ni_{0.6}Fe_2O_4$, the reagents were used as precursors are as follows: metal chlorides, cetyltrimethylammonium bromide (CTAB) as surfactant, sodium hydroxide and deionized water as solvent. Ferric chloride ($FeCl_3$), Nickel Chloride ($NiCl_2.6H_2O$) and Cadmium Chloride ($CdCl_2.2H_2O$) were used as product of Merck with purities exceeding 99% without further purification.

2.2 Synthesis procedure

Nanocrystalline particle $Ni_{0.6}Cd_{0.4}Fe_2O_4$ were synthesized by coprecipitation method in this work. This method provides advantages, such as low synthesis temperature, small particle size and easy to proceed. All of the chemicals used are analytical grade without further purification. For the synthesis of cadmium doped nickel ferrites nanoparticles, three solution containing 1 M solution of $FeCl_3$, 0.6 M solution of $NiCl_2.6H_2O$ and 0.4 M solution of $CdCl_2.H_2O$ were mixed and heated with continuous stirring for 30 min. pH of the mixed solution was maintained by aqueous solution of NaOH up to 11-12 range. Surfactant cetyltriammonuim bromide (CTAB), 0.5 g, was added to the mixed solution which was constantly stirred for 2 h so, obtained solution was aged at room temperature for 20 h. The precipitate was separated out and washed several times with distilled water in order to remove residual and impurities. The obtained product was dried in an oven at 100℃ for 3 h. The dried solid was crushed and crushed in a mortar to form powder. The obtained powder was calcined at 300℃ and other sample is not calcined.

3. CHARACTERIZATION TECHNIQUE

The XRD patterns of as prepared pure $Ni_{0.6}Cd_{0.4}Fe_2O_4$ and calcinated $Ni_{0.6}Cd_{0.4}Fe_2O_4$ nanoparticles were recorded on Pananalytical's X'Pert Pro X-ray diffractometer in the 2θ range 20 to 80° with step size of 0.025°. Scanning electron microscope (SEM) images of the prepared nanomaterial were observed on SEM Jeol equipment. The SEM micrographs were achieved at an operating voltage of 3 kV. EDX (Quantax 200 with X-Flash e Bruker) clearly identified the elements present in the nanoparticles. FTIR spectra of as prepared pure $Ni_{0.6}Cd_{0.4}Fe_2O_4$ and calcinated $Ni_{0.6}Cd_{0.4}Fe_2O_4$ samples were characterized by the Perkin Elmer Spectrum RXI in the range 4000-400 cm^{-1}. Photoluminescence spectral studies of the materials have been carried out on spectrofluorometer (Perkin Elmer LS 55) at excitation wavelength 262 nm is measure optical properties including band gap also. UV-Visible spectra were recorded in absorption mode on Cary 100 spectrophotometer in the wavelength region 200-800 nm.

4. RESULT AND DISCUSSION

4.1 Structural analysis

Fig. 1 (a, b) shows the XRD patterns of pure $Ni_{0.6}Cd_{0.4}Fe_2O_4$ and calcinated $Ni_{0.6}Cd_{0.4}Fe_2O_4$ samples, prepared by chemical coprecipitation methods. The structural analysis of the samples were made with the aid of X'pert software and the crystal structure of the samples was found to be inverse cubic spinel type. Using Scherer's equation, the average sizes of the crystals were estimated to be 9, 11 nm for pure

$Ni_{0.6}Cd_{0.4}Fe_2O_4$ and calicinated $Ni_{0.6}Cd_{0.4}Fe_2O_4$ sample. In the given XRD patterns, the value of 2θ at 30.40º, 36.42º, 43.97º, 48.02º, 56.49º, 62.03º and 66.41º corresponds to planes (220), (311), (400), (420), (333), (440) and (442) of the cubic Cd0.4Nio.6Fe2O4 as per JCPDS 790416. The value of lattice parameter (a) and the space group of this synthesized nanoparticles obtained from the XRD spectra are 8.394 Aº and F 43m (216).

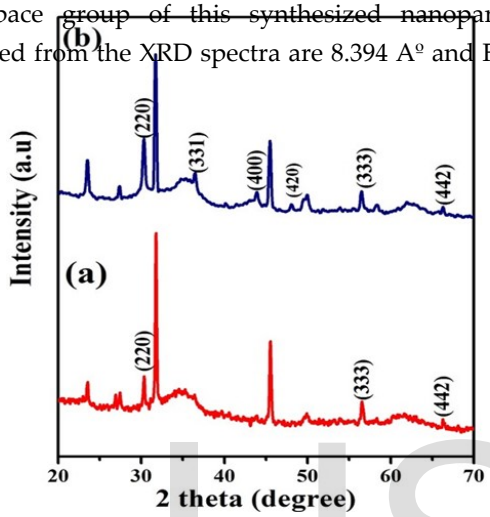

Figure: 1 XRD spectra (a) pure $Ni_{0.6}Cd_{0.4}Fe_2O_4$ (b) Calcinated $Ni_{0.6}Cd_{0.4}Fe_2O_4$

4.2 Morphological and elemental analysis

The morphology structure of the prepared ferrite nanoparticles is investigated by using SEM technique. Surface morphology of the prepared sample pure $Ni_{0.6}Cd_{0.4}Fe_2O_4$ and $Ni_{0.6}Cd_{0.4}Fe_2O_4$ are as revealed in Fig. 2 (a, b). SEM image of pure $Ni_{0.6}Cd_{0.4}Fe_2O_4$ sample demonstrate the formation of porous, microstructure, spongy and similar to network like structure are shown in Fig. 2. (a) and It can be observed that sample exhibit entirely interannular network with homogenous cavities and pores. In Fig. 2. (b) shows the nearly spherical morphology. The pores structure is accredited to the release of considerable amount of gases during calcination process. Fig. 2 (c, d) exhibit the EDX investigation of pure $Ni_{0.6}Cd_{0.4}Fe_2O_4$ and calcinated $Ni_{0.6}Cd_{0.4}Fe_2O_4$ nanoparticles carried out at room temperature for the elemental corroboration and purity of the sample. The EDX spectrum confirms the homogeneity and gradient of the elements Fe, O, Cd, Ni are present in the sample. The outcomes suggested that the precursors have completely reacted in the chemical reaction to form the single phase pure $Ni_{0.6}Cd_{0.4}Fe_2O_4$ and calcinated $Ni_{0.6}Cd_{0.4}Fe_2O_4$ nanoparticles as well as it approves that there is definitely not additional impurity existing in the samples. It is suggested that the comparative atomic mass ratio of the metal ferrites are acceptable matched along with the stoichiometry in preparation. The sample is gold coated for the improved visibility of the morphology shows in EDX spectra in form of peak.

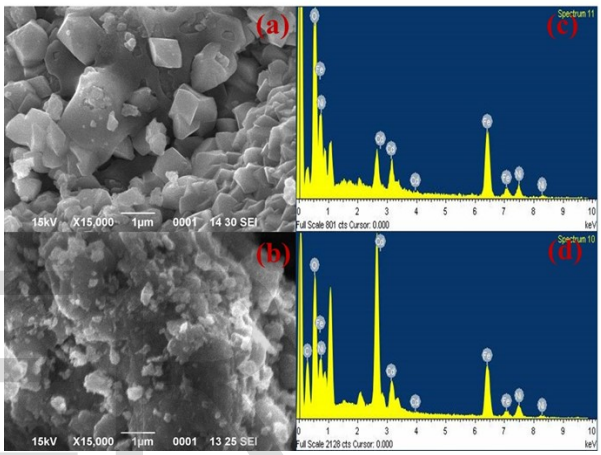

Figure: 2 SEM image (a) pure $Ni_{0.6}Cd_{0.4}Fe_2O_4$ (b) Calcinated $Ni_{0.6}Cd_{0.4}Fe_2O_4$ (c, d) EDX spectra of pure $Ni_{0.6}Cd_{0.4}Fe_2O_4$ and Calcinated $Ni_{0.6}Cd_{0.4}Fe_2O_4$

4.3 Functional analysis

FTIR spectrum of pure $Ni_{0.6}Cd_{0.4}Fe_2O_4$ and calcinated $Ni_{0.6}Cd_{0.4}Fe_2O_4$ at 400˚C for 4 h is shown in Fig. 3 (a, b). Spinel structure is confirmed by the most important absorption peak is detected in the range of 610-569 cm-1. This peak is apportioned to the intrinsic stretching vibration of bonds between Cd^{2+} and oxygen ions. Another weakest peak detected in the range of 460-480 cm-1 is assigned to the stretching vibration of bonds between Fe^{3+} 4O and Ni^{2+} 4O [15, 16]. A reduction in the wavenumber value of υ1 indicates that Cd^{2+} preferred tetrahedral sites involve sp^3 hybrid orbital and forms covalent bonds. Also Cd^{2+} pushes the Fe^{3+} ion to tetrahedral site owing to the higher atomic weight in assessment to Nickel and oxygen and affects the bond length of Fe^{3+} 4O. The increase in cadmium content influences the metal oxygen bonds in the A-sites is due to the transition between inverse and mixed spinel

structures. The absorption bands found at ~675 and ~1000-1300 cm^{-1} is assigned to the C-H group and C-O stretching bands correspondingly.

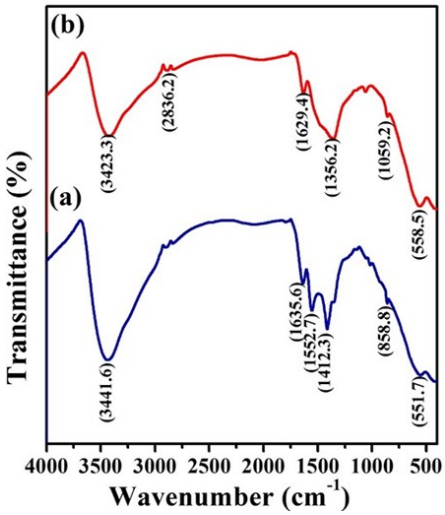

Figure: 3 FTIR spectra (a) pure $Ni_{0.6}Cd_{0.4}Fe_2O_4$ (b) Calcinated $Ni_{0.6}Cd_{0.4}Fe_2O_4$

4.4 OPTICAL ANALYSIS

4.4.1 Uv-visible spectroscopy

The optical properties were investigated by using UV-vis spectrophotometer for pure $Ni_{0.6}Cd_{0.4}Fe_2O_4$ and calcinated $Ni_{0.6}Cd_{0.4}Fe_2O_4$ ferrite nanoparticles as presented in Fig. 4 (a, b). In the condensed phase, Fe^{3+} exhibits three kinds of electronic transitions, first owing to ligand field transition, second owing to ligand metal charge transfer (LMCT from O^{2-} to Fe^{3+}) and third correspond to paired excitation of magnetically coupled Fe^{3+} ions occupying the adjacent sites in the crystals [17]. The band at 264 nm is accredited to Fe^{3+}←O charge transfer of isolated Fe ion in octahedral coordination [18]. The band at 373 nm is owing to charge transfer between oxygen and Fe^{2+} positioned in tetrahedral sites. Uninterrupted band gap energy of materials was calculated from the Tauc relation:

$$(\varepsilon h\nu)^2 = P\,(Eg - h\nu) \qquad \text{(Eq. 2)}$$

Where ε is the molar extinction coefficient, h is plank constant, ν is frequency of light, Eg is the band gap energy and P is the arbitrary constant. The linear part of the $(\varepsilon h\nu)^2$ verses hν graph (Fig. 4. a, b) was used to calculate the band gap values. The intercept of tangent at the x axis gives Eg value. The Eg values for the pure $Ni_{0.6}Cd_{0.4}Fe_2O_4$ and calcinated $Ni_{0.6}Cd_{0.4}Fe_2O_4$ materials 3.1, 3.2 eV using above relation.

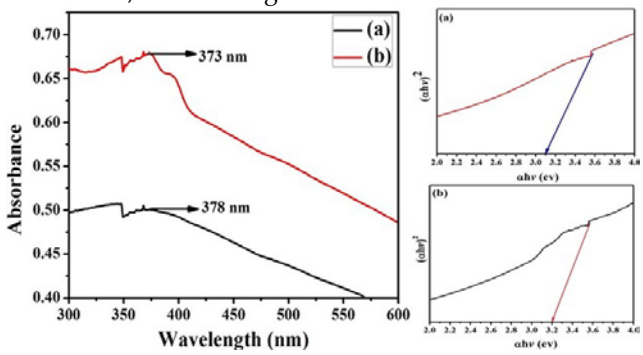

Figure: 4 Uv-visible spectra (a) pure $Ni_{0.6}Cd_{0.4}Fe_2O_4$ (b) Calcinated $Ni_{0.6}Cd_{0.4}Fe_2O_4$ and (a, b) band gap of pure $Ni_{0.6}Cd_{0.4}Fe_2O_4$ and calcinated $Ni_{0.6}Cd_{0.4}Fe_2O_4$

4.4.2 Fluorescence spectrophotometer

The photoluminescence spectra were recorded to investigate the recombination (or) effectiveness of photoproduced charge carrier, energetic situation of sub band gap and defects. Fig. 5 (a, b) shows the pure $Ni_{0.6}Cd_{0.4}Fe_2O_4$ and calicinated $Ni_{0.6}Cd_{0.4}Fe_2O_4$ ferrite system excited at 300 nm [20]. The peaks in the UV range at 432 nm outcomes from the recombination of a photoexcited electron from the valence band to conduction band and in circumstance of $NiFe_2O_4$ nanomaterial peak confirmations at 408 nm shows in fig.5 (b). The FL is accredited to lattice imperfections, and vacancies contained by the grain boundaries of pure ferrites system. The both samples appearance peak corresponding to violet emissions between 400-450 nm. The violet emissions are owing to the radiating imperfections correlated to the interface traps existing at grain restrictions [21]. The decrease in the luminescence concentration of calicinated $Cd_{0.6}Ni_{0.4}Fe_2O_4$ ferrites by increase the Cd^{2+} concentration, leads to intensification in the recombination rate of photogenerated electron-hole pairs. Thus, the FL can increases the photocatalytic property of calcinated $Ni_{0.6}Cd_{0.4}Fe_2O_4$ nanomaterial as compared to pure $Ni_{0.6}Cd_{0.4}Fe_2O_4$ material.

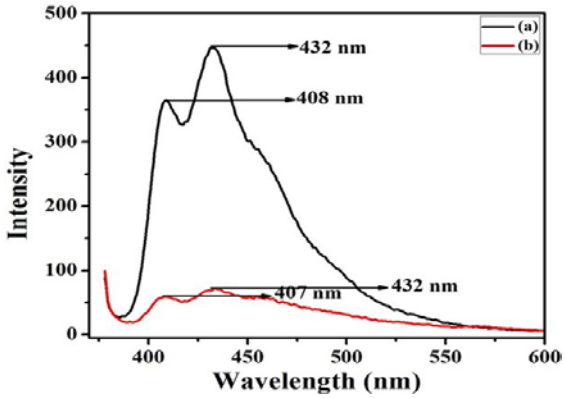

Figure: 5 PL spectra (a) pure $Ni_{0.6}Cd_{0.4}Fe_2O_4$ (b) Calcinated $Ni_{0.6}Cd_{0.4}Fe_2O_4$

5. CONCLUSION

In the present study I have synthesized cadmium doped nickel ferrite nanoparticles and calcinated for the effect of temperature on $Ni_{0.6}Cd_{0.4}Fe_2O_4$ by chemical coprecipitation method. From XRD pattern found cadmium doped nickel ferrite nanoparticles is cubic inverse spinel structure and match with JCPDS-790416 and SEM is used for the analysis of surface morphology and we found from sem image is pure $Ni_{0.6}Cd_{0.4}Fe_2O_4$ is network like structure and the surface of calcinated sample is nearly spherical shape and agglomerated type due to calcination temperature. For the analysis optical properties is used U.v-visible spectroscopy and Fluorescence spectra and the band gap is calculated from this spectra is 3.1, 3.2 eV for pure $Ni_{0.6}Cd_{0.4}Fe_2O_4$ and calcinated $Ni_{0.6}Cd_{0.4}Fe_2O_4$.

6. References

[1] Goldman A. Modern ferrite technology: Springer Science & Business Media; 2006.

[2] Sugimoto M. The past, present, and future of ferrites. Journal of the American Ceramic Society. 1999; 82:269-80.

[3] Kumar KV, Reddy ACS, Ravinder D. High-frequency dielectric behaviour of erbium substituted Ni-Zn ferrites. Journal of Magnetism and Magnetic Materials. 2003; 263:121-6.

[4] Deraz N, Alarifi A. Microstructure and magnetic studies of zinc ferrite nano-particles. Int J Electrochem Sci. 2012; 7:6501-11.

[5] Mirghni AA, Siddig MA, Omer MI, Elbadawi AA, Ahmed AI. Synthesis of $Zn_{0.5}CoxMg_{0.5-x}Fe_2O_4$ Nano-Ferrites Using Co-Precipitation Method and Its Structural and Optical Properties. American Journal of Nano Research and Applications. 2015; 3:27-32.

[6] Madhalea KV, Salunkhe MY, Bangale SV. Structural, morphological and hydrophilic properties of nanocrystalline $NiFe_2O_4$ by combustion route. Arch Appl Sci Res 2013; 5(1):62-7.

[7] Wolska E, Wolski W, Piszora P, Pietrusik M, Subrt J, Grygar T, et al. X-ray powder diffraction and Mossbauer studies on the formation of $Cd_{0.5}Ni_{0.5}$-$Fe_2O_4/Zn_{0.5}Ni_{0.5}Fe_2O_4$ spinel solid solutions. Int J Inorg Mater 1999; 1(2): 187-92.

[8] Gibbs TC. Principles of Mossbauer spectroscopy. London: Chapman and Hall; 1976. p. 22.

[9] Amer MA, Hemeda OM. Mossbauer and infrared studies of the system $Co_{1-x}Cd_xFe_2O_4$. J Phys Stat Sol B 1995; 96(1-2):99-109.

[10] Oak HN, Baek KS, Kim S. Mossbauer studies of superexchange interaction in € tetragonal $CuFe_2O_4$. J Phys Stat Sol B 1998; 208(1):249-55.

[11] Chinnasamy CN, Narayanasamy A, Ponpandian N, Chattopadhyay K, Shinoda K, Jeyadevan B, et al. Mixed spinel structure in nanocrystalline $NiFe_2O_4$. Phys Rev B 2001; 63:184108.

[12] Raghavender A, Kulkarni R, Jadhav K. Magnetic properties of nanocrystalline Al doped nickel ferrite synthesized by the sol-gel method. Chinese journal of physics. 2008; 46:366-75.

[13] Raghavender A.T., Kulkarni R.G., Jadhav K.M, Magnetic properties of nanocrystalline Al doped nickel ferrite synthesized by the sol-gel method, Chin. J. Phys. 46 (2008) 366-375.

[14] Mohammad Javad Nasr Isfahania, Parisa Nasr Isfahani, KlebsonLucenildo Da Silva, Armin Feldhoff, Vladimir Sepelak, Structural and magnetic properties of $NiFe_{2-x}Bi_xO_4$ (x= 0, 0.1, 0.15) nanoparticles prepared via solegel method, Ceram. Int. 37 (2011) 1905-1909.

[15] Chaudhari G.N., AC impedance spectroscopy study on nickel doped cadmium ferrites nano particles prepared by sol-gel citrate method, Int. J. Eng. Innov. Technol. 3 (2014) 167-170.

[16] Waldron R., Infrared spectra of ferrites, Phys. Rev. 99 (1955) 1727.

[17] Ladgaonkar B., Kolekar C., Vaingankar A., Infrared absorption spectroscopic study of Nd3þ substituted ZneMg ferrites, Bull. Mater. Sci. 25 (2002) 351-354.

[18] Pandey G. Fe–EBT Chelate Complex: A Novel Mean for Growth of α-FeOOH and γ-Fe_2O_3 Nanostructures. Acta Metallurgica Sinica (English Letters). 2014; 27:1127-33.

[19] Buvaneswari G, Aswathy V, Rajakumari R. Comparison of color and optical absorbance properties of divalent ion substituted Cu and Zn aluminate spinel oxides synthesized by combustion method towards pigment application. Dyes and Pigments. 2015; 123:413-9.

[20] Singh R, Narayan A, Prasad K, Yadav R, Pandey A, Singh A, et al. Thermal, structural, magnetic and photoluminescence studies on cobalt ferrite nanoparticles obtained by citrate precursor method. Journal of thermal analysis and calorimetry. 2012; 110:573-80.

[21] Selvam NCS, Vijaya JJ, Kennedy LJ. Comparative studies on influence of morphology and La doping on structural, optical, and photocatalytic properties of zinc oxide nanostructures. Journal of colloid and interface science. 2013; 407:215-24.